

## A NEW SHORT-CUT DESIGN METHOD FOR ULTRAFILTRATION AND HYPERFILTRATION CROSS-FLOW HOLLOW FIBER MEMBRANE MODULES

WAN RAMLI WAN DAUD<sup>1</sup>

**Abstract.** Although ultrafiltration and hyperfiltration have replaced many liquid phase separation equipment, both are still considered as “non-unit operation” processes because the sizing of both equipments could not be calculated using either the equilibrium stage, or the rate-based methods. Previous design methods using the dead-end and complete-mixing models are unsatisfactory because the dead-end model tends to underestimate the membrane area, due to the use of the feed concentration in the driving force, while the complete-mixing model tends to overestimate the membrane area, due to the use of a more concentrated rejection concentration in the driving force. In this paper, cross-flow models for both ultrafiltration and hyperfiltration are developed by considering mass balance at a differential element of the cross-flow module, and then integrating the expression over the whole module to get the module length. Since the modeling is rated-based, the length of both modules could be expressed as the product of the height of a transfer unit (HTU), and the number of transfer unit (NTU). The solution of the integral representing the NTU of ultrafiltration is found to be the difference between two exponential integrals ( $Ei(x)$ ) while that representing the NTU of hyperfiltration is found to be the difference between two hypergeometric functions. The poles of both solutions represent the flux extinction curves of ultrafiltration and hyperfiltration. The NTU for ultrafiltration is found to depend on three parameters: the rejection  $R$ , the recovery  $S$ , and the dimensionless gel concentration  $C_g$ . For any given  $C_g$  and  $R$ , the recovery,  $S$ , is limited by the corresponding flux extinction curve. The NTU for hyperfiltration is found to depend on four parameters: the rejection  $R$ , the recovery  $S$ , the polarization  $\beta$ , and the dimensionless applied pressure difference  $\psi$ . For any given  $\psi$  and  $R$ , the recovery,  $S$ , is limited by the corresponding flux extinction curve. The NTU for both ultrafiltration and hyperfiltration is found to be generally small and less than unity but increases rapidly to infinity near the poles due to flux extinction. Polarization is found to increase the NTU and hence the length and membrane area of the hollow fiber module for hyperfiltration.

**Keywords:** Ultrafiltration, hyperfiltration, reverse osmosis, hollow fiber module design, crossflow model, number of transfer unit, height of a transfer unit

### 1.0 INTRODUCTION

Although membrane processes for liquid separation such as ultrafiltration and hyperfiltration have replaced many other separation equipments in many industries, the process design of membrane modules, particularly cross flow modules such as the cross flow hollow fiber membrane modules, are still very empirical and not

<sup>1</sup> Department of Chemical and Process Engineering, Universiti Kebangsaan Malaysia 43600 UKM Bangi, Selangor, Malaysia. Email: wramli@eng.ukm.my

amenable to the normal unit operation design approach of using equilibrium stages or rates of mass transfer. This difficulty renders membrane processes as “non-unit operation” processes.

The previous design methods are only based on either complete-mixing [1-3] or dead-end models that mimic the experimental dead-end equipment for ultrafiltration and hyperfiltration systems [4-7]. These models for ultrafiltration and hyperfiltration suffer from various drawbacks, the most important of which is the increasing solute concentration along the tube, which in the case of ultrafiltration and hyperfiltration decreases the driving force for the solvent flux across the membrane further down the tube. This results in a smaller overall membrane area for the same separation duty compared to that predicted by the complete-mixing model, which uses the flux at the more concentrated retentate condition. The overall area is also bigger than that predicted by the dead-end model, which uses the flux at the more, dilute feed condition. The corresponding decrease in the rejection flow rate along the tube decreases the superficial velocity as well. The second major drawback is the pressure drop along the tube due to friction decreases the pressure difference along the tube that is available to drive the flux, resulting in a decrease in the flux across the membrane further down the tube. This again tends to decrease the overall size of the membrane area. In other words, the complete mixing model overestimates the area required while the dead end model underestimates the membrane area required for a given separation duty.

## 2.0 THE CROSS-FLOW MODEL DEVELOPMENT

### 2.1 Overall Solute and Solvent Balance

The fraction of the feed that is recovered in the permeate or recovery,  $S$ , is defined by

$$S = q_p / q_f \quad (1)$$

The fraction of the solute that is rejected,  $R_o$  is given by:

$$R_o = \frac{C_r - C_p}{C_r} = 1 - \frac{C_p}{C_r} \quad (2)$$

A solute mass balance at an infinitesimally small section of the membrane module  $dA$  of the cross-flow model as shown in Figure 1 yields:

$$qC = (q - dq_p)(C + dC) + dq_p C_p \quad (3)$$

Rearranging equation (4) and ignoring higher order terms gives:

$$-\frac{dq_p}{q} = \frac{dC}{(C_p - C)} \quad (4)$$

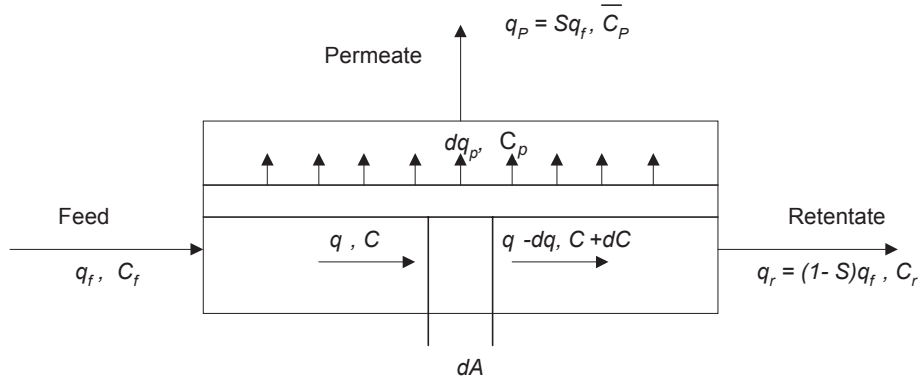


**Figure 1** Cross flow membrane module

The rejection  $R$  of the solute along the tube is assumed to be constant and is defined by:

$$R = \frac{C - C_p}{C} = 1 - \frac{C_p}{C} \quad (5)$$

By applying equation (5), the right hand side of equation (4) is replaced by:

$$\frac{dC}{(C_p - C)} = -\frac{dC}{CR} \quad (6)$$

The left hand side of equation (4) is replaced by virtue of equation (5) by:

$$-\frac{dq_p}{q} = -\frac{dS}{(1-S)} \quad (7)$$

Hence equation (4) becomes:

$$\frac{dC}{dS} = -\frac{CR}{(1-S)} \quad (8)$$

Mulder [5] obtained the same equation as equation (8) through a different route. The present derivation which was first derived earlier by Daud [8, 9] is more direct.

If this equation is integrated from  $C_f$  to  $C_r$ , then,

$$C_r = (1-S)^{-R} C_f \quad (9)$$

Hence the mean concentration of the permeate is given by:

$$\bar{C}_p = \frac{[1 - (1-S)^{1-R}]}{S} C_f \quad (11)$$

## 2.2 Volumetric Flow Rate and Solute Concentration Relationship

Before attempting to formulate and solve the rate based design equations, the relationship between the volumetric flow rate and the solute concentration in the tube must be established. Rearranging equations (4) and (6) then,

$$\frac{dq}{q} = -\frac{dC}{RC} \quad (12)$$

If equation (52) is integrated from  $C_f$ , to  $C$  and  $q_f$ , to  $q$ , then,

$$\ln(q/q_f) = -\frac{1}{R} \ln(C/C_f) \quad (13)$$

$$q/q_f = (C/C_f)^{-1/R} \quad (14)$$

If  $C = C_r$  and  $q = q_r$  and equation (1) is substituted in equation (14) then the latter reduces to equation (9). This shows that the derivation is consistent. Although Mulder[5] derived equation (8) using an integral balance, he did not go further to derive equation (12) and hence failed to get equation (13), which is crucial in solving the rate-based design.

## 2.3 Design Equations for the Cross Flow Ultrafiltration Membrane Module

The solvent mass balance across an infinitesimal area of the ultrafiltration membrane gives:

$$J\pi Dndx = \pi Dnk \ln\left(\frac{C_g}{C}\right) dx = dq_p \quad (15)$$

where  $n$  is the number of tubes, and  $D$  is the diameter of each tube. This equation could only be solved if the volumetric flow rate could be expressed in terms of the concentration. According to equations (12) and (14), the right hand side of equation (15) is given by:

$$dq_p = \frac{q}{RC} dC = \frac{q_f}{RC} \left(\frac{C}{C_f}\right)^{-1/R} dC = \frac{q_f}{RC_f^{-1/R}} C^{-(1+R)/R} dC \quad (16)$$

If equation (16) is substituted into equation (15), and the resulting equation is integrated from  $x = 0$  to  $x = L$  and from  $C = C_f$  to  $C = C_r$ , then,

$$L = \int_0^L dx = \frac{q_f}{\pi D n k R C_f^{-1/R}} \int_{C_f}^{C_r} \frac{C^{-(1+R)/R}}{\ln(C_g/C)} dC \quad (17)$$

The area of membrane required is given by:

$$A = \pi D n \int_0^L dx \frac{q_f}{k R C_f^{-1/R}} \int_{C_f}^{C_r} \frac{C^{-(1+R)/R}}{\ln(C_g/C)} dC \quad (18)$$

Equation (18) could be rewritten in terms of dimensionless variables.

$$\frac{A}{q_f/k} = \int_1^{C_r/C_f} \frac{(C/C_f)^{-(1+R)/R}}{R \ln[(C_g/C_f)/(C/C_f)]} d\left(\frac{C}{C_f}\right) \quad (19)$$

$$A = \int_1^{(1-S)^{-R}} \frac{C^{-(1+R)/R}}{R \ln[C_g/C]} dC \quad (20)$$

where  $A$  is the dimensionless area,  $C$  is the dimensionless solute concentration in the tube, and  $C_g$  is the dimensionless gel concentration given by:

$$A = \frac{A}{q_f/k} \quad C = \frac{C}{C_f} \quad C_g = \frac{C_g}{C_f} \quad (21)$$

Equations (17) and (18) could be rewritten in the NTU form by:

$$L = \left( \frac{q_f}{n \pi D k} \right) \int_1^{(1-S)^{-R}} \frac{C^{-(1+R)/R}}{R \ln[C_g/C]} dC = H_T N_T \quad (22)$$

where  $H_T$  is the height of a transfer unit based on the tube side given by:

$$H_T = \left( \frac{q_f}{n \pi D k} \right) \quad (23)$$

and  $N_T$  is the number of transfer unit based on the tube side given by:

$$N_T = \int_1^{(1-S)^{-R}} \frac{C^{-(1+R)/R}}{R \ln[C_g/C]} dC \quad (24)$$

Equation (24) indicates that the number of transfer unit for cross-flow ultrafiltration is dependent on 3 parameters,  $R$ ,  $S$ , and  $C_g$ .

#### 2.4 Design Equations for the Cross Flow Hyperfiltration Membrane Module Without Pressure Drop Along the Tube and Without Concentration Polarization

The solute mass balance across an infinitesimal area of the membrane is given by:

$$J\pi Dndx = \pi Dn(P/l)(\Delta P_T - iRRTC/M)dx = dq_p \quad (25)$$

If equations (16) is substituted into equation (25), and assuming that there is no pressure drop along the tube, the equation is integrated from  $x = 0$  to  $x = L$  and from  $C = C_f$  to  $C = C_r$  then,

$$L = \int_0^L dx = \frac{q_f}{\pi Dn(P/l)RC_f^{-1/R}} \int_{C_f}^{C_r} \frac{C^{-(1+R)/R}}{(\Delta P_T - iRRTC/M)} dC \quad (26)$$

The area of the membrane is given by:

$$A = \pi Dn \int_0^L dx = \frac{q_f}{(P/l)RC_f^{-1/R}} \int_{C_f}^{C_r} \frac{C^{-(1+R)/R}}{(\Delta P_T - iRRTC/M)} dC \quad (27)$$

Equation (27) could be cast in terms of dimensionless variables as follows:

$$\frac{A}{q_f/(P/l)\Delta P_T} \int_1^{C_r/C_f} \frac{(C/C_f)^{-(1+R)/R}}{R(1 - (iRRTC_f/M\Delta P_T)(C/C_f))} d\left(\frac{C}{C_f}\right) \quad (28)$$

$$A = \int_1^{(1-S)^{-R}} \frac{C^{-(1+R)/R}}{R(1 - RC/\psi)} dC \quad (29)$$

where  $\psi$  is the dimensionless applied pressure given by:

$$\psi = \frac{\Delta P_T}{iRRTC_f/M} \quad (30)$$

Equations (26) and (27) could be recast into the NTU form by:

$$L = \left( \frac{q_f}{n\pi D(P/l)\Delta P_T} \right) \int_1^{(1-S)^{-R}} \frac{C^{-(1+R)/R}}{R(1 - RC/\psi)} dC = H_T N_T \quad (31)$$

where  $H_T$  is the height of a transfer unit based on the tube side given by:

$$H_T = \left( \frac{q_f}{n\pi D (P/l) \Delta P_T} \right) \quad (32)$$

and  $N_T$  is the number of transfer unit based on the tube side given by:

$$N_T = \int_1^{(1-S)^{-R}} \frac{C^{-(1+R)/R}}{R(1-RC/\psi)} dC \quad (33)$$

Equation (33) indicates that the NTU of the cross-flow hyperfiltration module is dependent on 3 parameters  $R$ ,  $S$  and  $\psi$ .

## 2.5 Design Equations for the Cross Flow Hyperfiltration Membrane Module Without Pressure Drop Along the Tube and with Concentration Polarization

The solvent flux across a hyperfiltration membrane with concentration polarisation is given by:

$$J = (P/l) (\Delta P_T - i(\beta C - C_p) RT/M) \quad (34)$$

where  $\beta$  is the polarization coefficient. The solvent flux is given by:

$$\begin{aligned} J &= (P/l) (\Delta P_T - \Delta \Pi) = (P/l) (\Delta P_T - i(\beta C - C_p) RT/M) \\ &= (P/l) (\Delta P_T - i(R + \beta - 1) CRT/M) \end{aligned} \quad (35)$$

The solute mass balance across an infinitesimal area of the membrane is given by:

$$J\pi D n dx = \pi D n (P/l) (\Delta P_T - iRTC(R + \beta - 1)/M) dx = dq_p \quad (36)$$

If equation (16) is substituted into equation (36), and assuming that there is no pressure drop along the tube, the equation is integrated from  $x = 0$  to  $x = L$ , and from  $C = C_f$  to  $C = C_r$ , then,

$$L = \int_0^L dx = \frac{q_f}{\pi D n (P/l) RC_f^{-1/R}} \int_{C_f}^{C_r} \frac{C^{-(1+R)/R}}{(\Delta P_T - iRTC(R + \beta - 1)/M)} dC \quad (37)$$

The area of the membrane is given by:

$$A = \pi D n \int_0^L dx = \frac{q_f}{(P/l) RC_f^{-1/R}} \int_{C_f}^{C_r} \frac{C^{-(1+R)/R}}{(\Delta P_T - iRTC(R + \beta - 1)/M)} dC \quad (38)$$

Equation (38) could be cast in terms of dimensionless variables as follows:

$$\frac{A}{q_f / (P/l) \Delta P_T} \int_1^{C_r/C_f} \frac{(C/C_f)^{-(1+R)/R}}{R(1 - (iRTC_f / M\Delta P_T)(R + \beta - 1)C/C_f)} d\left(\frac{C}{C_f}\right) \quad (39)$$

$$A = \int_1^{(1-S)^{-R}} \frac{C^{-(1+R)/R}}{R(1 - (R + \beta - 1)C/\psi)} dC \quad (40)$$

Equations (37) could be recast into the NTU form by:

$$L = \left( \frac{\rho q_f}{n\pi D(P/l) \Delta P_T C_f} \right) \int_1^{(1-S)^{-R}} \frac{C^{-(1+R)/R}}{R(1 - (R + \beta - 1)C/\psi)} dC = H_T N_T \quad (41)$$

where  $H_T$  is the height of a transfer unit based on the tube side given by:

$$H_T = \left( \frac{q_f}{n\pi D(P/l) \Delta P_T} \right) \quad (42)$$

and  $N_T$  is the number of transfer unit based on the tube side given by:

$$N_T = \int_1^{(1-S)^{-R}} \frac{C^{-(1+R)/R}}{R(1 - (R + \beta - 1)C/\psi)} dC \quad (43)$$

Equation (43) indicates that the NTU of the cross-flow hyperfiltration module is dependent on 4 parameters,  $R$ ,  $S$ ,  $\beta$ , and  $\psi$ .

### 3. RESULTS AND DISCUSSION

#### 3.1 Ultrafiltration

Equation (24) for the NTU of the ultrafiltration membrane module can be integrated by first substituting  $z = \ln (C_g/C)/R$  is further substituted in equation (43), then it becomes:

$$N_T = \frac{C_g^{-1/R}}{R} \int_{\ln[C_g/(1-S)^{-R}]/R}^{\ln C_g/R} \frac{e^z}{z} dz \quad (44)$$



Finally, equation (44) can be expressed in terms of standard exponential integrals as

$$N_T = \frac{C_g^{-1/R}}{R} \left\{ \text{Ei}(\ln C_g / R) - \text{Ei} \left( \ln [C_g / (1-S)^{-R}] / R \right) \right\} \quad (45)$$

where

$$\text{Ei}(x) = \int_{-\infty}^x \frac{e^t}{t} dt \quad (46)$$

If the series expansion for this integral given by [10]:

$$\text{Ei}(x) = \gamma + \ln x + \sum_{n=1}^{\infty} \frac{x^n}{nn!} \quad (47)$$

where  $\gamma$  is the Euler constant, is substituted in equation (47) then,

$$N_T = \frac{C_g^{-1/R}}{R} \left\{ \ln \left( \frac{\ln C_g}{\ln [C_g / (1-S)^{-R}]} \right) - \sum_{n=1}^{\infty} \frac{\left\{ \ln [C_g / (1-S)^{-R}] / R \right\}^n - (\ln C_g / R)^n}{nn!} \right\} \quad (48)$$

Equation (48) was first derived by Daud[8]. It has a pole at

$$S = 1 - C_g^{-1/R} \quad (49)$$

$$R = -\ln C_g^{-\infty} / \ln(1-S) \quad (50)$$

corresponding to zero flux and  $N_T = \infty$ . Design charts of NTU for ultrafiltration hollow fiber module are shown in Figures 2 to 4.

Figures 2 to 4 show that the NTU for constant recovery,  $S$ , at first increases slowly as the rejection  $R$  is increased, and then increases sharply as the pole or the dimensionless gel concentration is reached, due the zero flux or flux extinction. The NTU value is generally less than 1.0 but increases sharply to infinity at the flux extinction point. At a lower value of the dimensionless gel concentration  $C_g$ , the poles or the flux extinction is reached much more quickly then at a larger  $C_g$ . As  $C_g$  is increased, the flux extinction is reached less quickly at the outlet and which for smaller  $S$  tends to be outside the domain of  $R$ . The NTU also increases as  $S$  is increased for all cases. The effect of the poles is to increase the NTU sharply near it. In other words, the length of the hollow fiber ultrafiltration module and therefore, the area required at the poles is very large. It

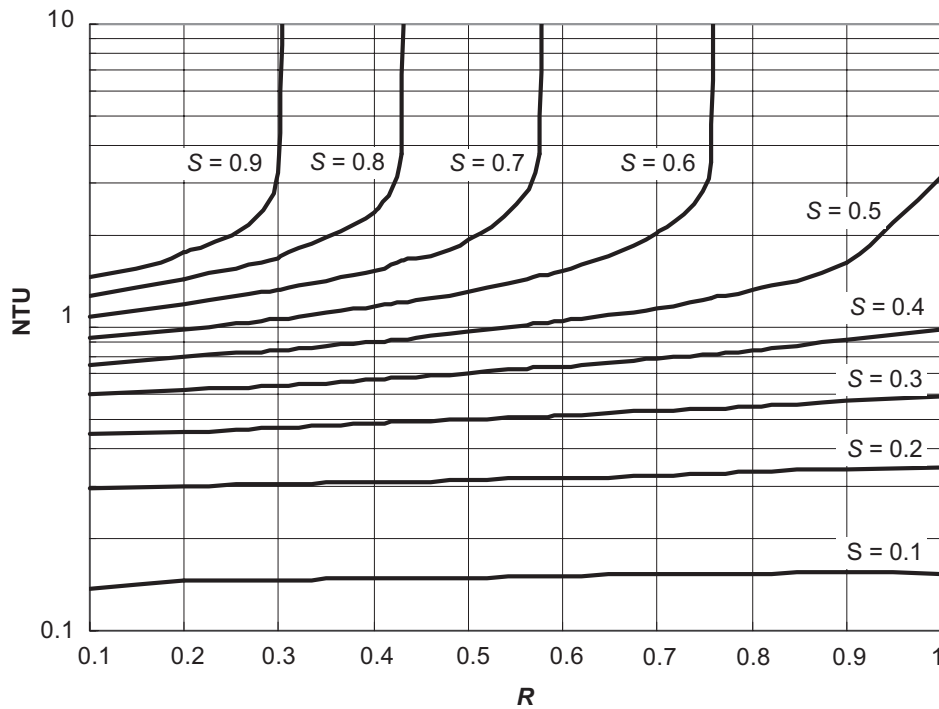


**Figure 2** Design chart for NTU of ultrafiltration hollow fibre module for  $C_g = 2$

implies that for very high rejection  $R$ , the operating point should be at a low  $S$  so that the area is not so large.

Not all possible pairs of values of rejection,  $R$ , and recovery,  $S$ , however, have NTU values due to the flux extinction. This effect can be seen clearly on the flux extinction curves [8] given by equation (49), which are plotted in Figure 5. The flux extinction curves represent the maximum attainable value of recovery,  $S$ , for any given  $C_g$  and  $R$ . It means that for any given  $C_g$  and  $R$ , the recovery,  $S$  is limited by the corresponding flux extinction curve. The flux extinction curves also show that the feasible value of recovery,  $S$ , is lower at lower values of  $C_g$  compared to that at higher  $C_g$ . Conversely, solutions with higher  $C_g$  can achieve higher rejection,  $R$ , and higher recovery,  $S$ , compared with those with a lower value of  $C_g$ . The NTU values are generally less than 1.0.

### 3.2 Hyperfiltration

Equation (43) for the  $N_T$  is the NTU of hyperfiltration reverse osmosis module can be integrated by first letting  $y = (1 - RC/\psi)$  such that,

$$N_T = -\frac{1}{R} \left( \frac{\psi}{R} \right)^{1/R} \int_{1-R/\psi}^{1-R(1-S)^{-R/\psi}} \frac{(1-y)^{-(1+R)/R}}{y} dy \quad (51)$$

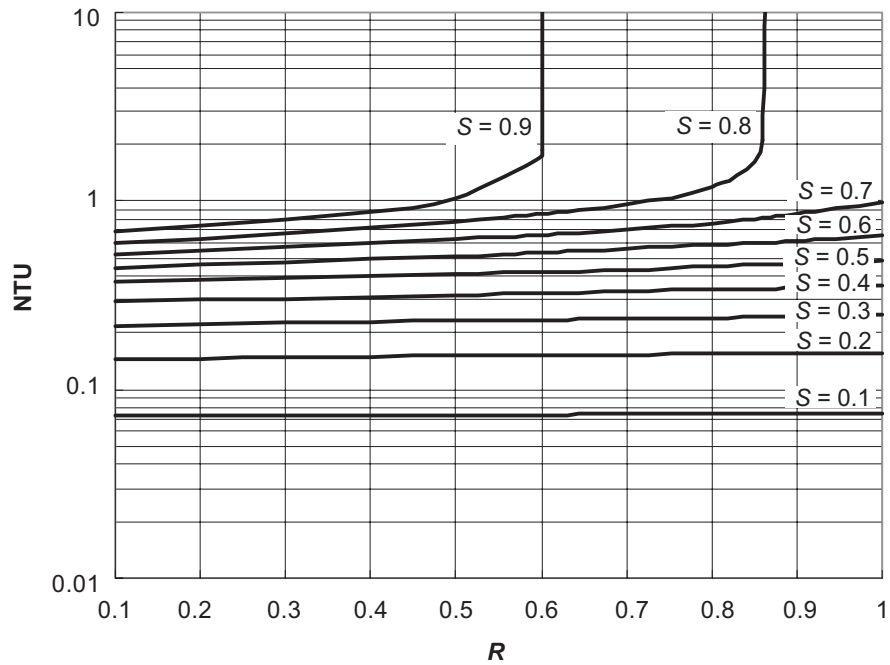


**Figure 3** Design chart for NTU of ultrafiltration hollow fibre module for  $C_g = 4$

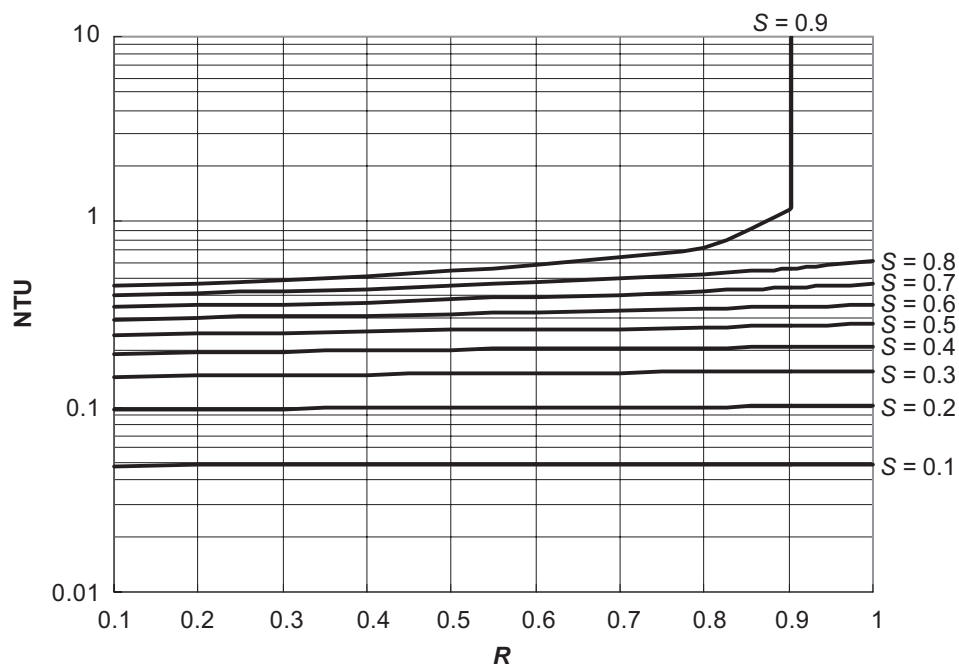


**Figure 4** Design chart for NTU of ultrafiltration hollow fibre module for  $C_g = 8$

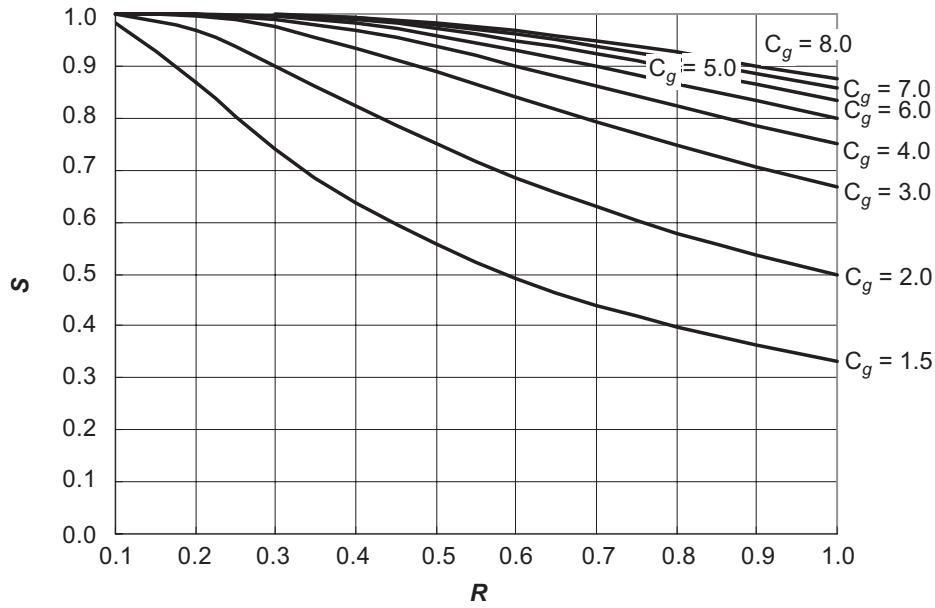


**Figure 5** The flux extinction curves of ultrafiltration

The integral in equation (91) can be repeatedly integrated by parts to yield:

$$\begin{aligned}
 \int \frac{(1-y)^{-(1+R)/R}}{y} dy &= R \left[ \frac{(1-y)^{-1/R}}{y} + \frac{R}{(1-R)} \left[ \frac{(1-y)^{-(1/R)/R}}{y^2} + \frac{R}{(1-2R)} \right. \right. \\
 &\quad \left. \left[ \frac{(1-y)^{-(1-2R)/R}}{y^3} \dots \dots \right. \right. \\
 &= \sum_{n=1}^{\infty} \frac{R^n (1-y)^{-(1-(n-1)R)/R}}{(1-(n-1)R)! y^n}
 \end{aligned} \tag{52}$$

The NTU for hyperfiltration is then given by:

$$\begin{aligned}
 N_T &= \left( \frac{\psi}{R} \right)^{-1/R} \sum_{n=1}^{\infty} \left\{ \frac{R^{n-1}}{(1-(n-1)R)!} \left[ \frac{(R/\psi)^{-(1-(n-1)R)/R}}{(1-R/\psi)^n} \right. \right. \\
 &\quad \left. \left. - \frac{[R(1-S)^{-R}/\psi]^{-(1-(n-1)R)/R}}{(1-R(1-S)^{-R}/\psi)^n} \right] \right\}
 \end{aligned} \tag{53}$$

Equation (53) was first derived by Daud[9]. It has two poles, one at  $R = \psi$ , which is beyond the domain of  $R$  and is therefore, non consequential and another at

$$R(1-S)^{-R} = \psi \quad (54)$$

corresponding to zero flux and  $N_T = \infty$ . Likewise, the NTU for hyperfiltration with concentration polarization is simply given by:

$$N_T = \left(\frac{\psi}{R}\right)^{-1/R} \sum_{n=1}^{\infty} \left\{ \frac{R^{n-1}}{(1-(n-1)R)!} \left[ \frac{((R+\beta-1)/\psi)^{=(1-(n-1)R)/R}}{(1-(R+\beta-1)/\psi)^n} - \frac{[(R+\beta-1)(1-S)^{-R}/\psi]^{-(1-(n-1)R)/R}}{(1-(R+\beta-1)(1-S)^{-R}/\psi)^n} \right] \right\} \quad (55)$$

The poles for equation (55) are at  $R = \psi + 1 - \beta$ , which is beyond the domain of  $R$  and is therefore, non consequential and at

$$(R+\beta-1)(1-S)^{-R} = \psi \quad (56)$$

corresponding to zero flux and  $N_T = \infty$ . The design charts for NTU versus  $R$  and  $S$  for various values of  $\psi$  are given in Figures 6 to 8.

The trend of the curves in Figures 6 to 8 follows generally those of ultrafiltration. They show that the NTU for constant recovery  $S$ , at first increases slowly as the rejection  $R$  is increased, and then increases sharply, the pole or applied pressure,  $\psi$  is reached due the zero flux or flux extinction. Likewise, the NTU value is generally less than 1.0 but increases sharply to infinity at the flux extinction point. At a lower value of the dimensionless applied pressure  $\psi$ , the pole or the flux extinction is reached much more quickly then at a larger  $\psi$ . As  $\psi$  is increased, the flux extinction is reached less quickly at the outlet and for which smaller  $S$  tends also to be outside the domain of  $R$ . The NTU also increases as  $S$  is increased for all cases. In other words, the length of the hollow fiber ultrafiltration module and therefore, the area required at the poles is very large. It implies that for very high rejection  $R$ , the operating point should be at a low  $S$ , so that the area is not so large.

Just as in the case of ultrafiltration, not all possible pairs of values of rejection,  $R$  and recovery,  $S$ , however, have NTU values due to the flux extinction. This effect can be seen clearly on the flux extinction curves[9] given by equation (54), which are plotted in Figure 9. The flux extinction curves represent the maximum attainable value of recovery,  $S$  for any given pair of  $\psi$  and  $R$ . It means that for any given  $\psi$  and  $R$ , the recovery,  $S$  is limited by the corresponding flux extinction curve. The flux extinction curves also show that the feasible value of recovery,  $S$  is lower at lower values of  $\psi$ ,

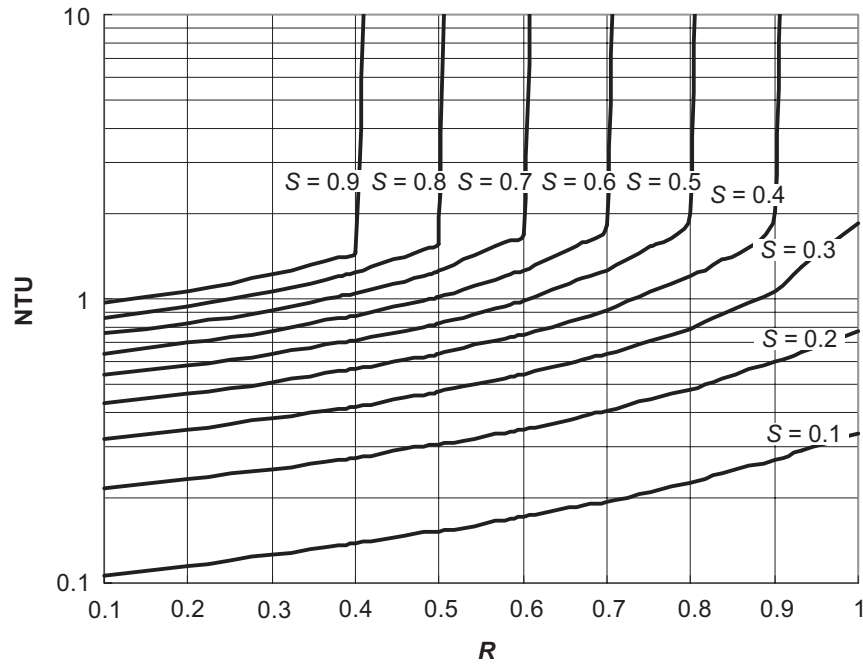


**Figure 6** Design chart for NTU of hyperfiltration hollow fiber module for  $\psi=1.5$

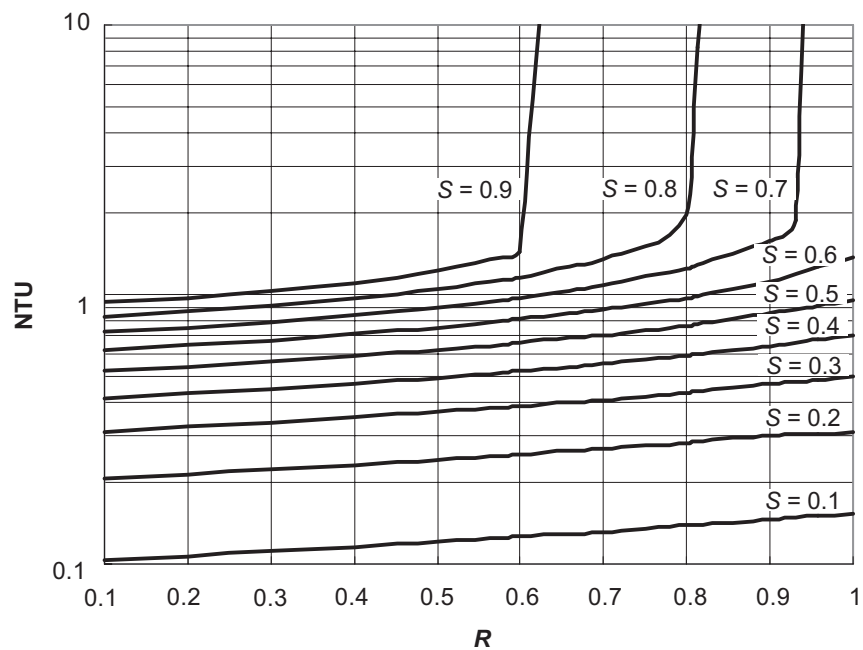


**Figure 7** Design chart for NTU of ultrafiltration hollow fiber module for  $\psi=3$

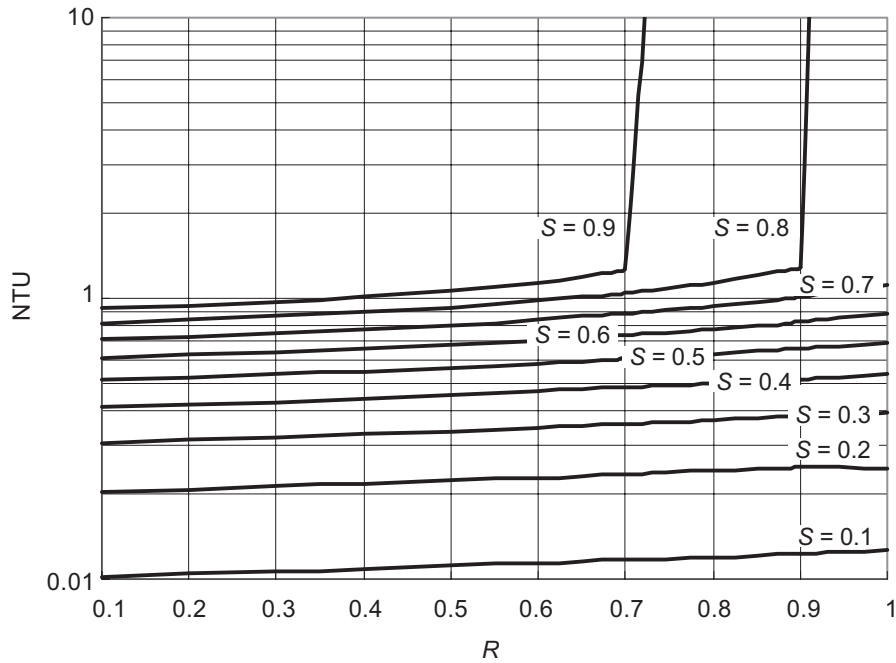


**Figure 8** Design chart for NTU of ultrafiltration hollow fiber module for  $\psi = 6$

compared to that at higher  $\psi$ . Conversely, hyperfiltration units with higher  $\psi$  can achieve higher rejection,  $R$  and higher recovery,  $S$ , compared with those with a lower value of  $\psi$ . The NTU values are generally small. The heights of a transfer unit are generally small with compared with those for ultrafiltration due to the smaller tube diameter used.

### 3.3 The effect of Polarization on Hyperfiltration Module Design

For most cases, polarization increases the rejection  $R$ , which becomes very close to unity. The NTU is also generally larger for the polarization cases. Hence both the membrane area and the module length are also generally larger as well for these cases. Polarization increases the osmotic pressure and therefore, decreases the driving force across the membrane. Therefore, a larger area is needed to effect the same separation for the same feed flow rate. The flux extinction curves for hyperfiltration given by equation (55) are plotted in Figure 10. It shows that polarization tends to lower the flux extinction curves because the polarized flux is smaller.

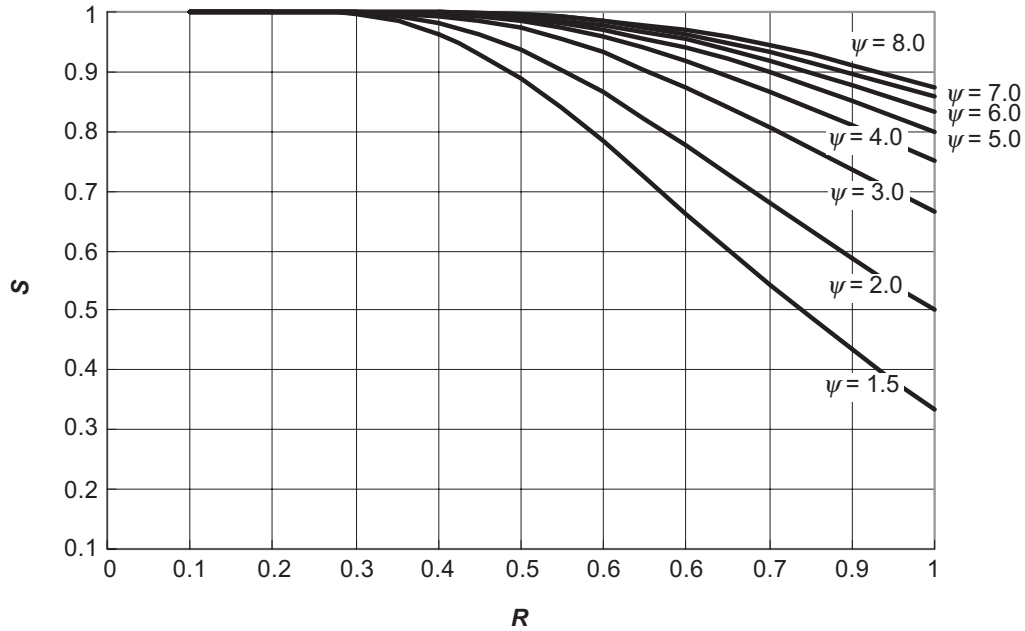


**Figure 9** The flux extinction curves of hyperfiltration without polarization

#### 4.0 CONCLUSIONS

It can be concluded that the length and the membrane area of hollow fiber modules for both ultrafiltration and hyperfiltration could be determined using the cross-flow model, whose solution could be expressed in terms of the NTU and HTU. The solution of the integral representing the NTU of ultrafiltration is found to be the difference between two exponential integrals (Ei), while that representing the NTU of hyperfiltration is found to be the difference between two hypergeometric functions. The poles of both solutions represent the flux extinction curves of ultrafiltration and hyperfiltration.

The NTU for ultrafiltration is found to depend on three parameters: the rejection  $R$ , the recovery  $S$ , and the dimensionless gel concentration  $C_g$ . For any given  $C_g$  and  $R$ , the recovery,  $S$  is limited by the corresponding flux extinction curve. The NTU for hyperfiltration is found to depend on four parameters: the rejection  $R$ , the recovery  $S$ , the polarization  $\beta$ , and the dimensionless applied pressure difference  $\psi$ . For any given  $\psi$  and  $R$ , the recovery,  $S$  is limited by the corresponding flux extinction curve. The NTU for both ultrafiltration and hyperfiltration is found to be generally small and less than unity but increases rapidly to infinity near the poles due to flux extinction. Polarization is found to increase the NTU, and hence the length and membrane area of the hollow fiber module for hyperfiltration.



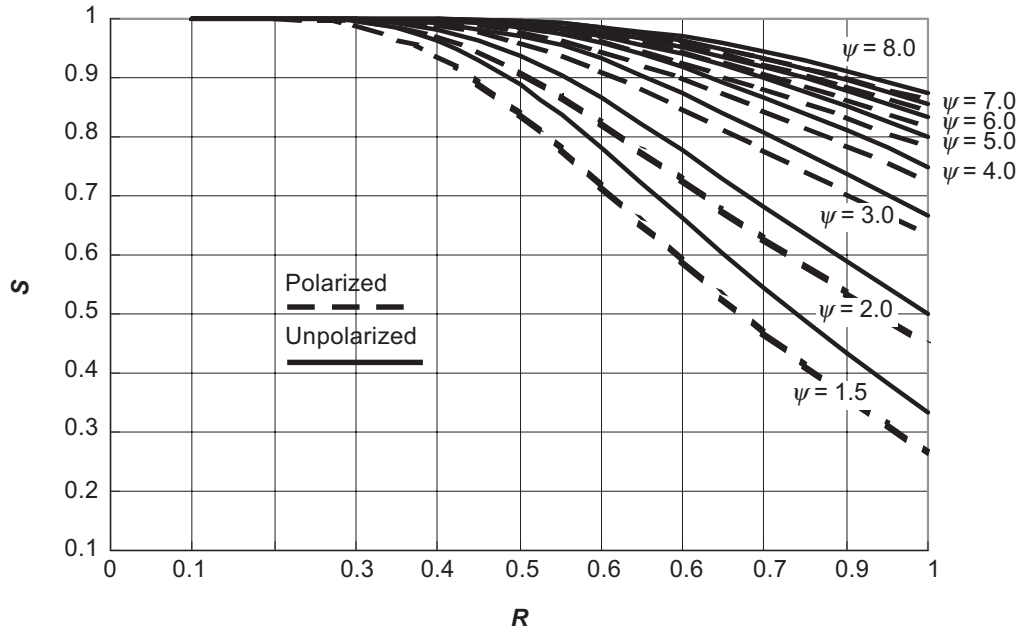


**Figure 10** The flux extinction curves of hyperfiltration module with polarisation ( $\beta = 1.105$ )

### ACKNOWLEDGEMENTS

I would like to thank Prof. Shaharir Mohamad Zain, Professor of Mathematics at the Center of Mathematical Science, Faculty of Science and Technology, Universiti Kebangsaan Malaysia for invaluable insights in the mathematics of this paper. I also would like to thank my colleague, Dr. Abdul Wahab Mohammad, for sparking my interest in membrane module design.

### NOMENCLATURE

$A$	membrane area
$A$	dimensionless membrane area
$C$	dimensionless solute concentration
$C$	solute mass concentration
$C_f$	feed solute concentration
$C_g$	dimensionless gel concentration
$C_g$	gel concentration
$C_p$	permeate solute concentration
$C_r$	retentate solute concentration

$D$	diameter of tube
$H_T$	height of a transfer unit
$i$	number of ion produced on solvation of the ionic solute
$J$	solvent flux
$J_s$	solute flux
$k$	mass transfer coefficient
$l$	membrane thickness
$L$	module length
$M$	solute molecular weight
$n$	number of tubes
$N_T$	number of transfer units
$\Delta P_T$	pressure drop across the membrane
$P$	solvent permeability coefficient
$P_s$	solute permeability coefficient
$q$	volumetric rate
$q_f$	feed volumetric rate
$q_p$	permeate volumetric flow rate
$q_r$	retentate volumetric flow rate.
$R$	rejection
$S$	recovery
$y$	dummy variable
$z$	dummy variable

### Greek letters

$\alpha$	membrane selectivity
$\beta$	polarization parameter
$\gamma$	Euler constant
$\Delta\Pi$	osmotic pressure difference
$\phi$	fraction of pores rejecting the solute
$\psi$	dimensionless applied pressure

## REFERENCES

- [1] Kimura, S., and S. Sourirajan. 1967. Analysis of Data in Reverse Osmosis with Porous Cellulose Acetate Membranes Used. *Amer. Inst. Chem. Eng. J.* 13: 497.
- [2] Hwang, S. T., and K. Kammermeyer. 1975. *Membranes in Separations*. New York: John Wiley.
- [3] Geankoplis, C. J. 1993. *Transport Processes and Unit Operations*. 3<sup>rd</sup> Edition. Englewood Cliffs. New Jersey: Prentice-Hall.
- [4] Wankat, P. C. 1990. *Rate-Controlled Separations*. New York: Elsevier Applied Science.
- [5] Mulder, M. 1991. *Basic Principles of Membrane Technology*. Dordrecht: Kluwer Academic Publishers.
- [6] Seader, J. D., and E. J. Henley. 1998. *Separation Process Principles*. New York: John Wiley and Sons, Inc.
- [7] Baker, R. W. 2000. *Membrane Technology and Applications*. New York: McGraw-Hill.
- [8] Daud, W. R. W. 2004. Rate-based Design of Non-fouled Cross-flow Hollow Fiber Membrane Modules for Ultrafiltration. *Separation Science & Technology*. 39(6): 1221–1238.
- [9] Daud, W. R. W. 2004. Rate-based Design of Non-fouled Cross-flow Hollow Fiber Membrane Modules for Hyperfiltration. *Chem. Eng. Res. & Des.* 82(8): 993 - 998.
- [10] Abramowitz, M., and I. A. Stegun. 1972. *Handbook of Mathematical Functions*. 9<sup>th</sup> printing. New York: Dover Publications Inc.